Inorganic Chemistry

Article

pubs.acs.org/IC

Dependence of the Photophysical Properties on the Number of 2,2′-Bipyridine Units in a Series of Luminescent Europium and Terbium Cryptates

Nicola Alzakhem, Caroline Bischof, and Michael Seitz*

Inorganic Chemistry I, Department of Chemistry and Biochemistry, Ruhr-University Bochum, 44780 Bochum, Germany

Supporting Information

ABSTRACT: The luminescence properties of a series of lanthanoid cryptates with an increasing number of 2,2′-bipyridine units have been investigated for the lanthanoids Eu and Tb in aqueous solution. The trends in important parameters that influence the photophysics in these complexes have been determined. With increasing bipyridine content, an increase is observed for the intersystem crossing efficiencies and the number of inner-sphere water molecules. In contrast, a decrease is found in the same direction for overall quantum yields, triplet energies, and sensitization efficiencies.

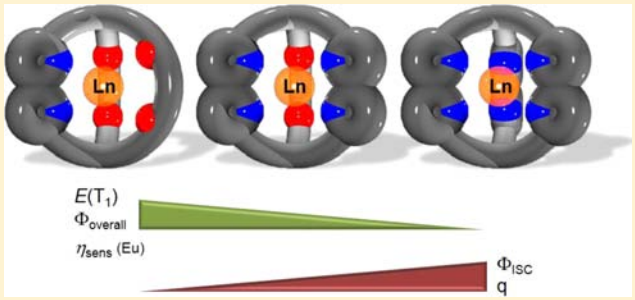

INTRODUCTION

Photoluminescence in molecular lanthanoid complexes has received a great deal of attention over the last decades because of their unique characteristics, making them vital components of many modern photonic applications.[1] The challenge for such complexes is the utilization of an appropriate ligand environment that is capable of populating lanthanoid emissive levels. This can be achieved through energy transfer from ligand-centered excited states. In addition, the ligand shields the lanthanoid center from deactivating, high-frequency oscillators such as water molecules. In 1987, Lehn et al. introduced a new class of luminescent lanthanoid complexes with 2,2′-bipyridine-based macrobicylic cryptands.[2] The initial report included the terbium(III) and europium(III) cryptates **Ln-1** with one 2,2′-bipyridine unit and a complementary nonphotoactive crown ether moiety, as well as the corresponding tris(2,2′-bipyridine) species **Ln-3** (Figure 1).

Despite the apparent similarity of the photoactive bipyridine moieties in all three cryptands, **Ln-1** and **Ln-3** showed significant differences in luminescence efficiency.[2a] For example in aqueous solution, the terbium complex **Tb-1** had a luminescence lifetime of τ_{obs} = 0.72 ms, while **Tb-3** exhibited a greatly reduced emission with τ_{obs} = 0.33 ms. At the time, this behavior was not commented on, and in subsequent publications, only the less luminescent tris(bipyridine) cryptates **Ln-3** were investigated in further detail[3] presumably due to their superior complex stability in biologically relevant media[4] and the naturally higher absorption coefficients compared to species with fewer bipyridine arms.

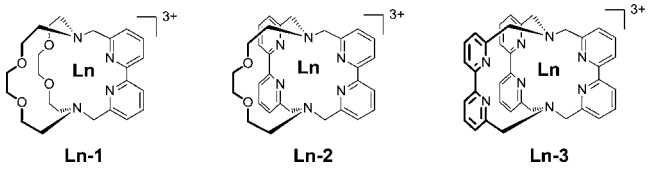

Figure 1. Known 2,2′-bipyridine-based lanthanoid cryptates **Ln-1** and **Ln-3** and new lanthanoid cryptate **Ln-2** with an intermediate number of bipyridine arms.

For the rational design of new and effective luminescence probes, it would be very helpful to have a detailed knowledge of how the different numbers of bipyridine chromophores in these cryptates change the various photophysical parameters that determine luminescence performance (intersystem crossing and energy transfer efficiencies, ligand triplet energies, lanthanoid radiative lifetimes, quantum yields, etc.). Continuing our previous work on bipyridine-based cryptates,[5] we have therefore undertaken a study in this context with the cryptates **Ln-1**, **Ln-2**, and **Ln-3** (Figure 1; Ln = Eu, Gd, Tb), which show a systematically increasing number of bipyridine units (from 1 to 3). We report here the synthesis of the previously unknown cryptates **Ln-2** and discuss the impact of the different numbers of bipyridine arms on the photophysical properties of this series.

RESULTS AND DISCUSSION

Synthesis of the Cryptates. All lanthanoid cryptates were prepared as the chloride species from the corresponding sodium complexes by metal exchange with the appropriate lanthanoid trichloride hexahydrates. The synthesis of **Na-1** was carried out following the pathway described in published articles[2a,6] (previously reported without synthetic details) starting from the commercially available aza-crown-ether **4**

Received: May 21, 2012
Published: August 21, 2012

dx.doi.org/10.1021/ic3010568 | Inorg. Chem. 2012, 51, 9343−9349

and 6,6′-bis(bromomethyl)-2,2′-bipyridine[7] (**5**) (Scheme 1). This method proved much less cumbersome than an earlier alternative route.[8] **Na-3** and the complexes **Ln-3** were prepared by a published procedure.[9]

Scheme 1. Synthesis of the Lanthanoid Cryptates Ln-1

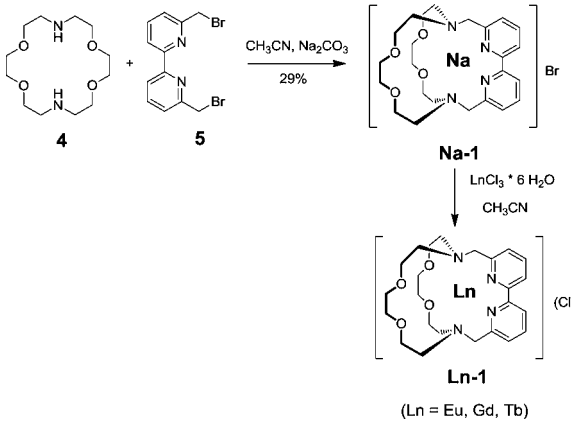

The synthesis of the unknown sodium cryptate **Na-2** was first attempted by the reaction of the bis(bipyridine) macrocycle **6**[10] (Scheme 2) with the triethylene glycol derivative **7**[11] under

Scheme 2. Attempted Synthesis of the Sodium Cryptate Na-2

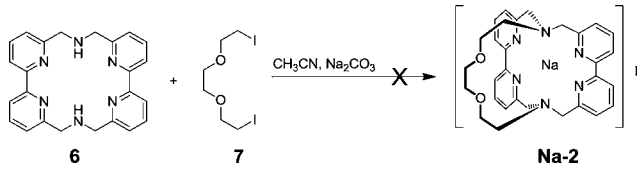

standard high-dilution and sodium-templating conditions. Unfortunately, this macrobicyclization reaction, which generally gives only low to modest yields, did not even provide the corresponding sodium cryptate **Na-2** in trace amounts. Instead, a different synthetic route involving the novel macrocycle **11** (Scheme 3) proved to be successful. The synthesis of **11** was achieved starting from 6,6′-bis(hydroxymethyl)-2,2′-bipyridine (**8**).[12] Swern oxidation[13] to the corresponding dialdehyde **9**[14] followed by a magnesium-templated macrocyclization/reduction sequence (used in the past for a similar compound[15]) with commercially available 1,8-diamino-3,6-dioxaoctane (**10**) yielded **11** in 53% yield over three steps. Macrobicyclization with 6,6′-bis(bromomethyl)-2,2′-bipyridine[7] (**5**) under standard, nonoptimized conditions (Na_2CO_3, CH_3CN, high dilution) gave **Na-2** in low yield (17%).

Single-Crystal X-ray Crystallography. Single-crystal X-ray analysis was possible on the sodium cryptate **Na-1** after crystallization of its methanolic solutions by slow evaporation. The asymmetric unit contains two very similar, independent cryptates, both showing an eight-coordinate sodium center with all available donor atoms bound to the metal center (Figure 2).

The sodium cations are well separated from the bromide counteranions (minimal distance Br2−Na2 = 5.88 Å) and do not bind additional external ligands. This situation is completely analogous to the one previously described for the sodium complex with the cryptand [phen·phen·phen], which consists of three phenanthroline arms and which is structurally a very good model for the tris(bipyridine) ligand in **Na-3**.[17]

Scheme 3. Synthesis of the Lanthanoid Cryptates Ln-2

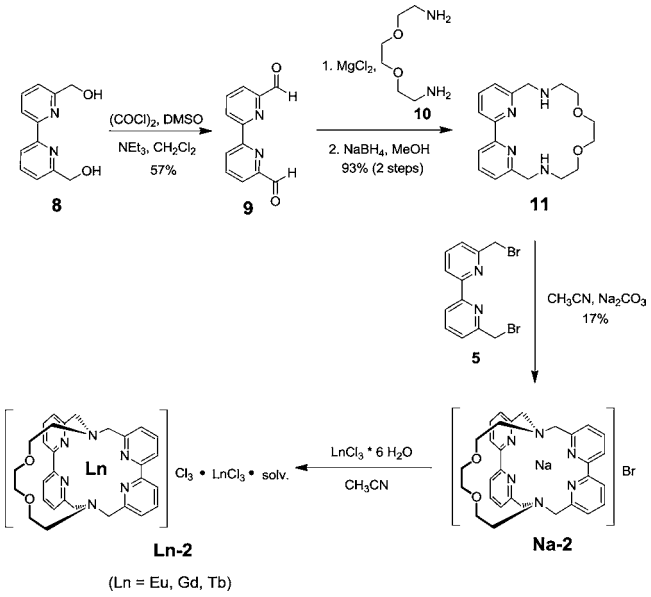

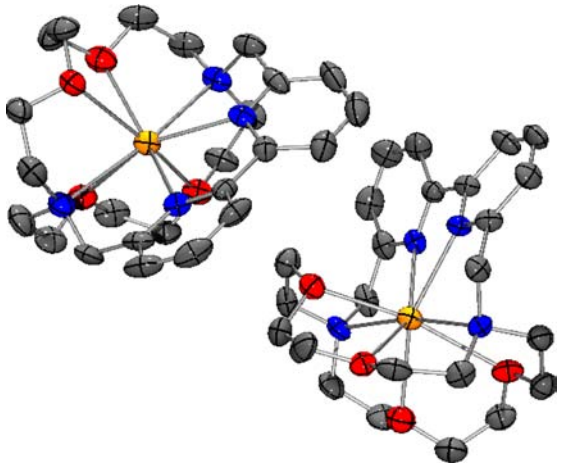

Figure 2. Thermal ellipsoid plot for the two independent sodium cryptate cations **Na-1** in the asymmetric unit (Ortep 3 for Windows,[16] 50% probability level). The hydrogen atoms, the free bromide anions, and the isolated water molecules are omitted for clarity. Color scheme: C, gray; N, blue; O, red; Na, orange.

One important difference between the cryptate structures in **Na-1** and the sodium complex with [phen·phen·phen] is the flexibility of the ligand arms. [phen·phen·phen] is very rigid and enforces a rather long, average bond length between Na and the six aromatic nitrogen donors of the phenanthroline units (av N_{ar}−Na = 2.70 Å).[17] In contrast, the crown ether arms in **Na-1** are capable of wrapping flexibly around the metal, which permits a closer approach of the metal to the bipyridine nitrogens (av N_{ar}−Na = 2.61 Å).

The situation in the corresponding lanthanoid cryptates is different. The crystal structure of **Tb-3** was previously reported to exhibit external ligands (one chloride and one water molecule) in the inner coordination sphere of the metal center.[18] This binding of additional ligands seems to be valid for the entire series **Ln-1**, **Ln-2**, and **Ln-3** (see luminescence lifetime measurements in H_2O and D_2O). This is not surprising, considering the much higher Lewis acidity of

dx.doi.org/10.1021/ic3010568 | Inorg. Chem. 2012, 51, 9343−9349

trivalent lanthanoid cations compared to monocationic sodium centers.

Photophysical Properties. The Eu and Tb complexes with the same cryptand show very similar absorption spectra in aqueous solution (Figures 3 and 4). The spectral features,

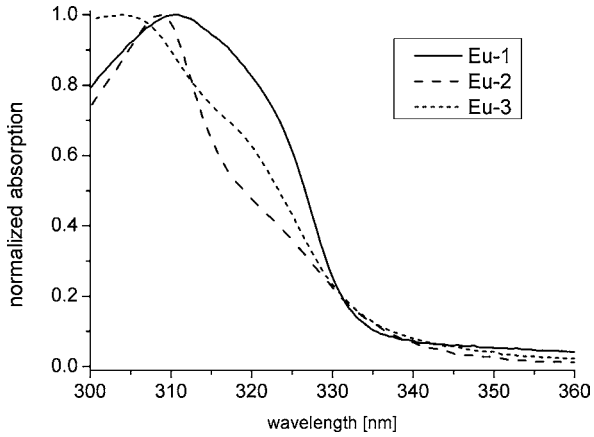

Figure 3. Absorption spectra of **Eu-1**, **Eu-2**, and **Eu-3** (tris buffer, pH 6.8).

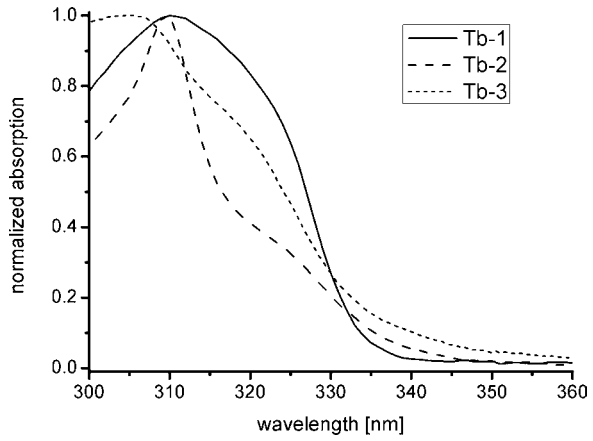

Figure 4. Absorption spectra of **Tb-1**, **Tb-2**, and **Tb-3** (tris buffer, pH 6.8).

however, change considerably with the use of different cryptands. **Ln-1** exhibits a broad unstructured band with a maximum at 311 nm. With an increasing number of bipyridines in **Ln-2** and **Ln-3**, the absorption maxima shift to shorter wavelengths (**Ln-2**: 309 nm; **Ln-3**: 304 nm) and show more pronounced shoulders around 320−325 nm.

The steady-state emission spectra after excitation close to the absorption maxima in aqueous solutions show the typical bands for the lanthanoids Eu and Tb (Figures 5 and 6). In the case of the terbium cryptates, the differences are only marginal. In contrast, the spectra for the europium species expectedly show changes along the cryptate series due to the generally higher sensitivity of europium bands to the coordination environment. Notably, only one single peak is found in the europium spectra for each $^5D_0 \rightarrow {}^7F_0$ band (which theoretically involves only nondegenerate levels and is therefore not supposed to be showing any crystal field splitting), suggesting the presence of one single species in all cases (at least on the time scale of the measurement). In addition, the same transitions show a progressive increase in relative intensity going from **Eu-3** via

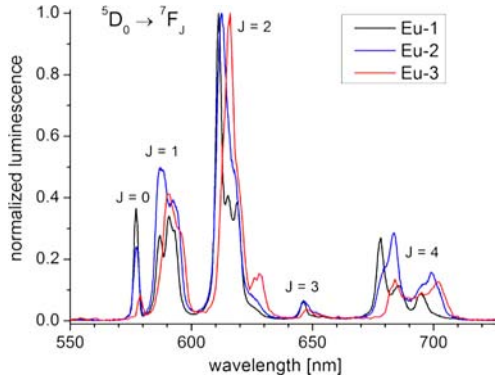

Figure 5. Steady-state emission spectra for **Eu-1**, **Eu-2**, and **Eu-3** (λ_{exc} = 313 nm, tris buffer, pH 6.8).

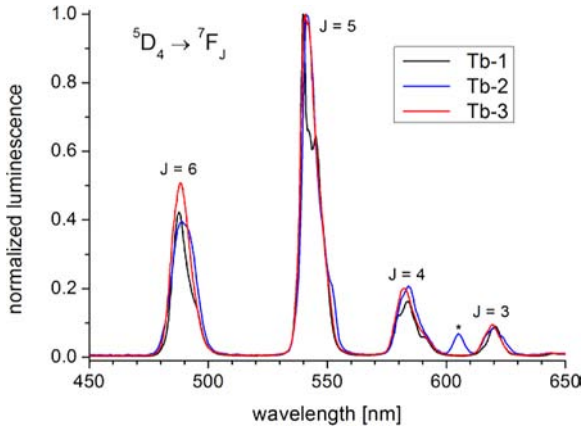

Figure 6. Steady-state emission spectra for **Tb-1**, **Tb-2**, and **Tb-3** (λ_{exc} = 306 nm, tris buffer, pH 6.8) (* second-order excitation peak).

Eu-2 to **Eu-1**. This trend seems to indicate a decreasing level of symmetry in the same direction, because this transition is only allowed in coordination environments with low symmetry around the europium cation.

The positions of the ligand-centered triplet levels (T_1) were measured by low-temperature emission spectroscopy of the gadolinium cryptates (Figure 7, Table 1). The zero-phonon $T_1 \rightarrow S_0$ transition energy, $E(T_1)$, was determined by fitting the structured phosphorescence bands with a series of Gaussians (see Figures S1−S3 in the Supporting Information). In our

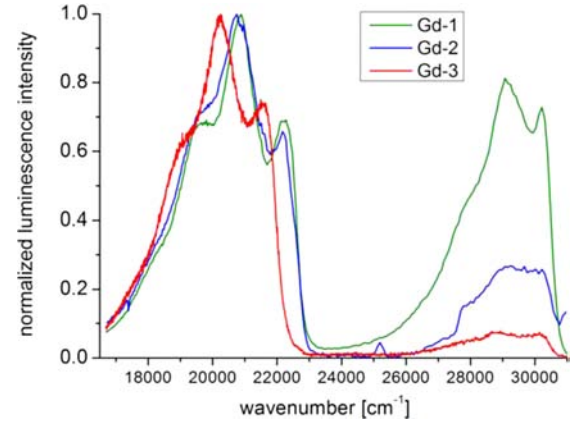

Figure 7. Low-temperature (77 K) steady-state emission spectra of **Gd-1**, **Gd-2**, and **Gd-3** (λ_{exc} = 304 nm, MeOH/EtOH, 1:1, v/v).

dx.doi.org/10.1021/ic3010568 | Inorg. Chem. 2012, 51, 9343−9349

Table 1. Ligand-Centered Zero-Phonon $T_1 \rightarrow S_0$ Transition Energy, $E(T_1)$, in the Gadolinium Complexes

entry	complex	$E(T_1)$ [cm^{-1}]
1	**Gd-1**	22 200
2	**Gd-2**	22 200
3	**Gd-3**	21 600

hands, **Gd-3** exhibits a value $E(T_1)$ = 21 600 cm^{-1}, which is in excellent agreement with previous measurements.[3d] As concluded in earlier reports, this energy level lies too close to the emitting level for Tb ($^5D_4$ at ca. 20 500 cm^{-1})[19] to prevent energy back-transfer onto the ligand and concomitant loss of sensitization efficiency.[3d] Remarkably, the two other gadolinium cryptates **Gd-1** and **Gd-2** show a substantially higher triplet level (both at $E(T_1)$ = 22 200 cm^{-1}). This helps to reduce the detrimental impact of the energy back-transfer mechanism as in **Gd-3** and should therefore yield higher luminescence efficiencies. In contrast to the situation for Tb, all three triplet energies are sufficiently above the emitting level of Eu (mainly $^5D_0$ at ca. 17 300 cm^{-1})[19] to rule out back-transfer, again a fact that has been established before for **Eu-3**.[3d] The fluorescent transitions from the first excited singlet state S_1 to the ground state S_0 (around 29 000 cm^{-1}) show an interesting trend (Figure 7). With increasing number of bipyridine units (**Gd-1** via **Gd-2** to **Gd-3**), the intensity of this band steadily decreases in comparison to ligand phosphorescence. This indicates an enhancement of intersystem crossing (ISC) ($S_1 \rightarrow T_1$) in the same direction. It has been reported before that ISC efficiencies in **Ln-3** are close to unity (e.g., >95% for **Tb-3**[3b,d]). The situation, however, that this phenomenon seems to be connected to the number of bipyridine arms has not been realized before.

Luminescence lifetimes were determined in H_2O and D_2O at ambient temperature. For the terbium complexes, where **Tb-3** is known to be susceptible to quenching by O_2 due to the low-lying T_1 states,[3b,d] the measurements were performed on degassed solutions (sparging with dioxygen-free N_2). From the lifetime differences, the number of inner-sphere water molecules q was evaluated using the empirical equations introduced by Beeby et al.[20] For the europium cryptates **Eu-1** and **Eu-2**, better shielding of the metal was observed compared to **Eu-3**, as indicated by smaller q values (Table 2: 1.9/2.1 vs 2.5). Presumably, this is due to the greater flexibility of the ethylene ether bridges compared to the rather stiff bipyridine arms (see crystal structure for **Na-1**). These occupy much more space around the europium centers, leading to a decrease of available free coordination sites for water molecules. This trend should also be found in the terbium complexes because of the very similar ionic radii of Eu and Tb. The q values vary widely (Table 2: **Tb-1**, 0.9; **Tb-2**, 2.0; **Tb-3**, 4.4). The unrealistically high value for **Tb-3** is most likely due the fact that there is considerable energy back-transfer because of the low triplet level (see above). This has been pointed out before in a similar case.[21] In addition, it has been noted before that the empirical equations, which are usually established using structurally characterized lanthanoid complexes with DOTA-derived or aminocarboxylate ligands, do not adequately describe the situation for lanthanoid bipyridine-based cryptates.[22]

Quantum yields of the europium and terbium cryptates were measured in aqueous solutions for Tb and Eu. For both lanthanoids, the quantum yields for **Ln-1** are approximately twice as high as for the corresponding complexes **Ln-2** and **Ln-3** (Table 2; Eu: 5.2% vs 2.4%/2.0% and Tb: 6.8% vs 3.7%/3.4%). In order to get further insight into the various parameters that determine luminescence efficiency, the data for the cryptates **Eu-(1−3)** were examined in more detail. Europium is a special case among the lanthanoids because according to Judd−Ofelt theory it is relatively straightforward to determine the radiative lifetime τ_{rad} from the emission spectra using the special properties of the magnetic-dipole-allowed transition $^5D_0 \rightarrow {}^7F_1$.[23] This approach is probably more reliable than the previous determination of τ_{rad} in **Eu-3** by assuming that the real radiative lifetime is equal to the observed lifetime in D_2O at low temperature (77 K).[3c,d] The latter method gave a radiative lifetime τ_{rad} = 1.7 ms for **Eu-3**,[3c,d] whereas the Judd−Ofelt approach yields substantially higher values of τ_{rad} = 6.2−8.1 ms for **Eu-(1−3)** (Table 2). With the calculated radiative lifetimes, the intrinsic quantum yields Φ_{Ln}^{Ln} for **Eu-(1−3)** were established using the equation displayed in Table 2. While a trend toward lower intrinsic quantum yields appears to be present going from **Eu-1** (6.3%) via **Eu-2** (5.4%) to **Eu-3** (4.2%), the relatively large uncertainties of the calculated values preclude conclusive statements. Using the intrinsic quantum yields Φ_{Ln}^{Ln} in combination with the measured absolute quantum yields Φ_{L}^{Ln}, however, gives significant differences in the sensitization efficiencies, η_{sens} (Table 2): **Eu-1** (83%) via **Eu-2** (44%) to **Eu-3** (48%). η_{sens} is mainly reflecting ISC and energy transfer from the ligand-centered triplet state to the lanthanoid. The qualitative result (vide infra) that ISC efficiencies seem to increase with an increasing number of bipyridine rings (see Figure 7) would suggest a concomitant rise in η_{sens}. Since the opposite effect is actually observed, i.e., **Eu-3** having a low value for η_{sens}, the energy transfer efficiencies would consequently have to decrease in the direction **Eu-3** via **Eu-2** to **Eu-1** in order to be able to explain the measured data.

Table 2. Luminescence Data for the Lanthanoid Complexes Ln-1, Ln-2, and Ln-3 in H_2O and D_2O

entry	complex	λ_{abs} [nm]	τ_{H_2O} [ms]	τ_{D_2O} [ms]	q[d]	τ_{rad} [ms]	$\Phi_{Ln}^{Ln} = \frac{\tau_{H_2O}}{\tau_{rad}}$	Φ_{L}^{Ln}	η_{sens}
1	**Eu-1**	311	0.39	1.3	1.9	6.2[g]	0.063	0.052	0.83
2	**Eu-2**	309	0.34	1.1	2.1	6.3[g]	0.054	0.024	0.44
3	**Eu-3**	304	0.34[c]	1.7[c]	2.5	8.1[f,g]	0.042	0.020[c]	0.48
4	**Tb-1**[a]	311[b]	1.3	1.9	0.90			0.068[b]	
5	**Tb-2**[a]	309[b]	0.42	0.52	2.0			0.037[b]	
6	**Tb-3**[a]	304[b]	0.44	0.75	(4.4)[e]			0.034[b]	

[a]Degassed solutions, λ_{exc} = 306 nm, λ_{em} = 542 nm. [b]In 0.5 mM tris buffer (pH 6.8). [c]See refs 3c and 3d. [d]q = number of inner-sphere water molecules; see ref 20. [e]Equation for the calculation of q not applicable. [f]See ref 3c. [g]Calculated using the equation $1/\tau_{rad} = A_{MD,0} n^3 (I_{tot}/I_{MD})$; see ref 23.

dx.doi.org/10.1021/ic3010568 | Inorg. Chem. 2012, 51, 9343−9349

In summary, the following trends in important photophysical parameters are observed when increasing the number of bipyridine units in the cryptates **Ln-(1−3)**: (i) an increase in the energy of the first excited singlet state S_1; (ii) a lowering of the T_1 triplet energy levels combined with an increase in ISC efficiencies; (iii) an increase in the number of bound solvent molecules; and (iv) a decrease in overall quantum yields for both Eu and Tb, with the cryptates **Ln-1** being approximately twice as emissive as **Ln-2** and **Ln-3**, the latter two being very similar.

For the europium cryptates, the following additional phenomena can be seen: While the radiative lifetimes and the intrinsic quantum yields are similar for all three cryptates **Eu-(1−3)** within the limits of the uncertainties, the sensitization efficiencies, η_{sens}, deteriorate with increasing number of bipyridine units. This trend seems to be connected to a concomitant decrease in energy transfer efficiencies from the ligand to the metal.

EXPERIMENTAL SECTION

General Procedures. 1,8-Diamino-3,6-dioxaoctane (**10**) and 1,4,7,10-tetraoxa-7,16-diazacyclooctadecane (**4**) (Kryptofix 22) were purchased from Merck KGaA (Darmstadt, Germany). Anhydrous $MgCl_2$ was purchased from Sigma-Aldrich. 6,6′-Bis(hydroxymethyl)-2,2′-bipyridine (**8**),[12] 6,6′-bis(bromomethyl)-2,2′-bipyridine (**5**),[7] and the cryptates **Ln-1**/**Ln-3** (Ln = Eu, Gd, Tb)[6] were prepared according to previously reported procedures. CH_3CN for the synthesis of the cryptates was HPLC-grade. Other solvents were dried by standard procedures (MeOH: Mg/I_2; NEt_3 and CH_2Cl_2: CaH_2). Air-sensitive reactions were carried out under a dry, dioxygen-free atmosphere of N_2 using Schlenk techniques. Column chromatography was performed with silica gel 60 (Merck KGaA, 0.063−0.200 mm). Analytical thin layer chromatography was done on silica gel 60 F_{254} plates (Merck, coated on aluminum sheets). ESI mass spectrometry was measured using Bruker Daltonics Esquire6000. NMR spectra were measured on a Bruker DPX-250 (^{1}H: 250 MHz, ^{13}C: 62.9 MHz) and DPX-200 (^{1}H: 200 MHz). UV/vis spectra were recorded on a Jasco-670 spectrophotometer using 1.0 cm quartz cuvettes.

Photophysical Measurements. Steady-state emission spectra at room temperature were acquired on a PTI Quantamaster QM4 spectrofluorimeter using 1.0 cm quartz cuvettes. The excitation light source was a 75 W continuous xenon short arc lamp. Emission was monitored at 90° using a PTI P1.7R detector module (Hamamatsu PMT R5509-72 with a Hamamatsu C9525 power supply operated at −1500 V and a Hamamatsu C9940 liquid N_2 cooling unit set to −80 °C). Where applicable, solutions were degassed by sparging with dry, dioxgen-free N_2. Low-temperature spectra were recorded on frozen glasses of solutions of the gadolinium complexes (MeOH/EtOH, 1:1, v/v) in standard NMR tubes using a dewar cuvette filled with liquid N_2 (T = 77 K). Spectral selection was achieved by single grating monochromators (excitation: 1200 grooves/mm, blazed at 300 nm; visible emission: 1200 grooves/mm, blazed at 400 nm). Luminescence lifetimes were determined with the same instrumental setup. The light source for these measurements was a xenon flash lamp (Hamamatsu L4633: 10 Hz repetition rate, pulse width ca. 1.5 μs fwhm). Lifetime data analysis (deconvolution, statistical parameters, etc.) was performed using the software package FeliX32 from PTI. Lifetimes were determined either by fitting the middle and tail portions of the decays or by deconvolution of the decay profiles with the instrument response function, which was determined using a dilute aqueous dispersion of colloidal silica (Ludox AM-30). The estimated uncertainties in τ_{obs} are ±10%. All measured values are averages of three independent experiments.

X-ray Analysis. A colorless block of **Na-1** having approximate dimensions of 0.5 × 0.3 × 0.2 mm^3 was mounted on a glass fiber using perfluoropolyether oil. The measurement was carried out on a Bruker Smart 1000 CCD diffractometer using graphite-monochromated Mo Kα radiation. Data were collected at a temperature of 233(2) K. Frames corresponding to an arbitrary hemisphere of data were collected using ω scans. The structure was solved within the Wingx[24] package using direct methods (SIR92[25]) and expanded using Fourier techniques (SHELXL-97[26]). The hydrogen atoms were included but not refined. They were positioned geometrically, with distances C−H = 0.93 Å for aromatic hydrogens and C−H = 0.97 Å in all benzylic and aliphatic positions. All hydrogens were constrained to ride on their parent carbon atoms. U_{iso}(H) values were set at 1.2 times U_{eq}(C).

Crystallographic data for **Na-1**: chemical formula $C_{24}H_{34}BrN_4NaO_6$, formula weight 577.45, T = 233(2) K, λ = 0.71073 Å, triclinic, space group $P\bar{1}$, a = 12.046(5) Å, b = 15.136(6) Å, c = 17.045(7) Å, α = 113.260(8)°, β = 96.789(9)°, γ = 102.264(9)°, V = 2718(2) Å^3, Z = 4, μ = 1.572 mm^{-1}, $R(F_o)$ = 0.1160, $R_w(F_o^2)$ = 0.3073, GOF = 0.964.

Synthesis of Na-1. Under N_2 1,4,7,10-tetraoxa-7,16-diazacyclooctadecane (**4**) (90 mg, 342 μmol, 1.0 equiv) was dissolved in CH_3CN (200 mL, HPLC grade), and Na_2CO_3 (363 mg, 3.4 mmol, 10 equiv) was added. The suspension was heated to reflux, and a solution of 6,6′-bis(bromomethyl)-2,2′-bipyridine (**5**) (117 mg, 342 μmol, 1.0 equiv) in CH_3CN (250 mL, HPLC grade) was added under high-dilution conditions over 16 h. The mixture was heated under reflux for an additional 18 h, cooled to ambient temperature, and filtered. The filtrate was concentrated under reduced pressure, and the resulting residue was subjected to column chromatography (SiO_2, gradient: CH_2Cl_2/MeOH, 100:1 → 25:1) to yield the title compound as a colorless solid (54 mg, 29%). Single crystals suitable for X-ray analysis were grown by slow evaporation of solutions of the title compound in moist MeOH.

^{1}H NMR (250 MHz, $CDCl_3$): δ 7.91−7.79 (m, 4 H), 7.37−7.27 (m, 2 H), 3.78 (s, 4 H), 3.71−3.37 (m, 16 H), 2.88−2.69 (m, 4 H), 2.67−2.48 (m, 4H) ppm. ^{13}C NMR (62.9 MHz, $CDCl_3$): δ 158.7, 155.5, 138.6, 124.2, 120.9, 68.5, 66.4, 59.9, 53.4.

Synthesis of Dialdehyde 9. Under N_2 and at −60 °C, oxalyl chloride (452 mg, 0.30 mL, 3.56 mmol, 2.2 equiv) was dissolved in CH_2Cl_2 (20 mL), and a solution of dry DMSO (556 mg, 7.12 mmol, 4.4 equiv) in dry CH_2Cl_2 (5 mL) was added. The mixture was stirred for 5 min at this temperature before a solution of 6,6′-bis-(hydroxymethyl)-2,2′-bipyridine (**8**) (350 mg, 1.62 mmol, 1.0 equiv) in CH_2Cl_2 (50 mL, with a minimum of dry DMSO necessary to dissolve everything) was added dropwise. After 15 min, dry NEt_3 (16.2 mmol, 1.63 g, 2.26 mL, 10 equiv) was added, and the mixture was allowed to reach room temperature over the course of ca. 5 h. Water (75 mL) was added, the phases were separated, and the aqueous layer was extracted with CH_2Cl_2 (2 × 50 mL). After drying the combined organic phases ($MgSO_4$), the solvent was removed under reduced pressure and the remaining light brown solid was subjected to column chromatography (SiO_2, CH_2Cl_2/MeOH, 24:1, detection: UV). The product was isolated as a colorless solid (196 mg, 57%). The analytical data of the product were in agreement with previous reports using different synthetic procedures.[14]

^{1}H NMR (200 MHz, $CDCl_3$): δ 10.19 (s, 2 H), 8.85−8.81 (m, 2 H), 8.07−8.02 (m, 4 H) ppm.

Synthesis of Macrocycle 11. Under N_2, anhydrous $MgCl_2$ (88 mg, 0.92 mmol, 1.0 equiv) and 2,2′-bipyridine-6,6′-dicarbaldehyde (**9**) (196 mg, 0.92 mmol, 1.0 equiv) were suspended in dry MeOH (20 mL), and the mixture was stirred at room temperature for 30 min. 1,8-Diamino-3,6-dioxaoctane (**10**) (137 mg, 0.92 mmol, 1.0 equiv) in dry MeOH (2 mL) was added, stirring was continued for 1 h, and $NaBH_4$ (4.62 mmol, 175 mg, 5.0 equiv) was added in small portions. After 20 h at room temperature, water (20 mL) was added to the clear solution, MeOH was removed under reduced pressure, and the aqueous phase was extracted with CH_2Cl_2 (3 × 35 mL). The combined organic layers were dried ($MgSO_4$) and concentrated. The crude product (280 mg, 93%) was obtained as a faintly yellow oil that appears to be slightly air-sensitive. It was therefore stored under inert atmosphere at 4 °C and was used without further purification.

^{1}H NMR (250 MHz, $CDCl_3$): δ 8.41−7.06 (m, 4 H), 7.35−7.06 (m, 2 H), 4.04−3.85 (m, 4 H), 3.72−3.52 (m, 8 H), 2.94−2.74 (m, 4 H) ppm. ^{13}C NMR (62.9 MHz, $CDCl_3$): δ 159.7, 159.1, 158.9, 156.6, 137.1, 137.0, 122.2, 122.0, 120.6, 119.3, 70.8, 70.6, 70.3, 64.2, 55.0,

dx.doi.org/10.1021/ic3010568 | Inorg. Chem. 2012, 51, 9343−9349

54.9, 49.0, 48.8. MS (ESI+): m/z (%) 351.13 (100, $[M + Na]^+$), 329.18 (13, $[M + H]^+$).

Synthesis of Na-2. Macrocycle **11** (132 mg, 402 μmol, 1.0 equiv) was dissolved in CH_3CN (200 mL), and anhydrous Na_2CO_3 (426 mg, 4.02 mmol, 10 equiv) was added. The suspension was heated to reflux, and a solution of 6,6′-bis(bromomethyl)-2,2′-bipyridine (**5**) (137 mg, 402 μmol, 1.0 equiv) in freshly distilled CH_3CN (300 mL) was added under high-dilution conditions over 9 h. The mixture was heated under reflux for an additional 20 h, cooled to ambient temperature, and filtered. The filtrate was concentrated under reduced pressure. The residue was subjected to column chromatography (SiO_2, gradient: CH_2Cl_2/MeOH 24:1 → 9:1, detection: UV and I_2 vapor). The product was isolated as a colorless solid (42 mg, 17%).

^{1}H NMR (250 MHz, $CDCl_3$): δ 8.03−7.81 (m, 8 H), 7.43−7.33 (m, 4 H), 3.97 (d, J = 14.0 Hz, 4 H), 3.82−3.61 (m, 12 H), 2.72 (t, J = 5.2 Hz, 4 H) ppm. ^{13}C NMR (62.9 MHz, $CDCl_3$): δ 158.8, 155.6, 138.7, 124.7, 120.8, 69.0, 66.1, 59.9, 53.3 ppm. MS (ESI+): m/z (%) 531.13 (100, $[M]^+$). R_f = 0.17 (SiO_2, CH_2Cl_2/MeOH, 9:1, detection: UV and I_2 vapor).

Synthesis of Ln-2. General procedure: A solution of **Na-2** (1.0 equiv) and $LnCl_3{\cdot}6H_2O$ (1.05 equiv) in dry acetonitrile was heated under reflux overnight. The solvent was removed in vacuo. The remaining residue was dissolved in a minimum amount of MeOH, and the solution was layered with Et_2O. After storing the suspension at room temperature overnight, the precipitate was collected on a membrane filter (nylon, 0.45 μm), washed with Et_2O, and dried in vacuo to yield the lanthanoid complex as a light yellow powder.

Eu-2: 1.4 mg (from 10.8 mg of **Na-2**). MS (ESI+): m/z (%) 730.93 ($[M + 2Cl]^+$). Anal. Calcd (Found) for $[C_{30}H_{32}N_6O_2Eu](Cl)_3{\cdot}EuCl_3{\cdot}H_2O{\cdot}3MeOH{\cdot}Et_2O$ (M_r = 1213.52): C, 36.6 (36.9); H, 4.65 (4.79); N, 6.93 (7.34).

Gd-2: 5.1 mg (from 10.1 mg of **Na-2**). MS (ESI+): m/z (%) 735.94 ($[M + 2Cl]^+$). Anal. Calcd (Found) for $[C_{30}H_{32}N_6O_2Gd](Cl)_3{\cdot}GdCl_3{\cdot}8H_2O$ (M_r = 1179.95): C, 30.5 (30.0); H, 4.10 (3.75); N, 7.12 (6.78).

Tb-2: 2.7 mg (from 7.1 mg of **Na-2**). MS (ESI+): m/z (%) 736.85 ($[M + 2Cl]^+$). Anal. Calcd (Found) for $[C_{30}H_{32}N_6O_2Tb](Cl)_3{\cdot}TbCl_3{\cdot}4H_2O$ (M_r = 1111.24): C, 32.4 (32.1); H, 3.63 (4.04); N, 7.56 (8.16).

■ ASSOCIATED CONTENT

Ⓢ Supporting Information

Gaussian fits for the triplet levels in **Gd-(1−3)**. Crystallographic information file for **Na-1**. This material is available free of charge via the Internet at http://pubs.acs.org.

■ AUTHOR INFORMATION

Corresponding Author

*E-mail: michael.seitz@rub.de.

Notes

The authors declare no competing financial interest.

■ ACKNOWLEDGMENTS

M.S. thanks Prof. Dr. Nils Metzler-Nolte (Ruhr-University Bochum) for his continued support. The authors thank Dr. Klaus Merz (Ruhr-University Bochum) for help with the crystal structure measurement. Financial support is gratefully acknowledged from DFG (Emmy Noether Fellowship to M.S.), Fonds der Chemischen Industrie (Liebig Fellowship to M.S. and predoctoral fellowships for N.A.), Int. Max Planck Research School in Chemical Biology (Predoctoral fellowship for C.B.), and Research Department Interfacial Systems Chemistry (Ruhr-University Bochum). C.B. is grateful for support by the Ruhr-University Research School.

■ REFERENCES

(1) Selected reviews: (a) *Lanthanide Luminescence* (Springer Series on Fluorescence 7); Hänninen, P.; Härma, H., Eds.; Springer: Berlin, 2011. (b) Bünzli, J.-C. G. *Chem. Rev.* **2010**, *110*, 2729−2755.

(2) (a) Alpha, B.; Lehn, J.-M.; Mathis, G. *Angew. Chem., Int. Ed. Engl.* **1987**, *26*, 266−267. (b) Alpha, B.; Balzani, V.; Lehn, J.-M.; Perathoner, S.; Sabbatini, N. *Angew. Chem., Int. Ed. Engl.* **1987**, *26*, 1266−1267.

(3) Review: (a) Sabbatini, N.; Guardigli, M.; Lehn, J.-M. *Coord. Chem. Rev.* **1993**, *123*, 201−228. Selected original articles: (b) Blasse, G.; Dirksen, G. J.; Sabbatini, N.; Perathoner, S.; Lehn, J.-M.; Alpha, B. *J. Phys. Chem.* **1988**, *92*, 2419−2422. (c) Blasse, G.; Dirksen, G. J.; van der Voort, D.; Sabbatini, N.; Perathoner, S.; Lehn, J.-M.; Alpha, B. *Chem. Phys. Lett.* **1988**, *146*, 347−351. (d) Alpha, B.; Ballardini, R.; Balzani, V.; Lehn, J.-M.; Perathoner, S.; Sabbatini, N. *Photochem. Photobiol.* **1990**, *52*, 299−306. (e) Prodi, L.; Maestri, M.; Balzani, V.; Lehn, J.-M.; Roth, C. *Chem. Phys. Lett.* **1991**, *180*, 45−50. (f) Cross, J. P.; Dadabhoy, A.; Sammes, P. G. *J. Lumin.* **2004**, *110*, 113−124. (g) Guillaumont, D.; Bazin, H.; Benech, J.-M.; Boyer, M.; Mathis, G. *ChemPhysChem* **2007**, *8*, 480−488.

(4) Mathis, G.; Bazin, H. In *Lanthanide Luminescence* (Springer Series on Fluorescence 7); Hänninen, P.; Härma, H., Eds.; Springer: Berlin, 2011; pp 47−88.

(5) (a) Bischof, C.; Wahsner, J.; Scholten, J.; Trosien, S.; Seitz, M. *J. Am. Chem. Soc.* **2010**, *132*, 14334−14335. (b) Doffek, C.; Alzakhem, N.; Molon, M.; Seitz, M. *Inorg. Chem.* **2012**, *51*, 4539−4545.

(6) Mathis, G.; Lehn, J.-M. Patent US4927923, May 22, 1990.

(7) Newkome, G. R.; Kiefer, G. E.; Kohli, D. K.; Xia, Y.-J.; Fronczek, F. R.; Baker, G. R. *J. Org. Chem.* **1989**, *54*, 5105−5110.

(8) Buhleier, E.; Wehner, W.; Vögtle, F. *Chem. Ber.* **1978**, *111*, 200−204.

(9) Rodriguez-Ubis, J.-C.; Alpha, B.; Plancherel, D.; Lehn, J.-M. *Helv. Chim. Acta* **1984**, *67*, 2264−2269.

(10) Newkome, G. R.; Pappalardo, S.; Gupta, V. K.; Fronczek, F. R. *J. Org. Chem.* **1983**, *48*, 4848−4851.

(11) Crossley, R.; Goolamali, Z.; Gosper, J. J.; Sammes, P. G. *J. Chem. Soc., Perkin Trans. 2* **1994**, 513−520.

(12) Newkome, G. R.; Puckett, W. E.; Kiefer, G. E.; Gupta, V. K.; Xia, Y.; Coreil, M.; Hackney, M. A. *J. Org. Chem.* **1982**, *47*, 4116−4120.

(13) Omura, K.; Swern, D. *Tetrahedron* **1978**, *34*, 1651−1660.

(14) 2,2′-Bipyridine-6,6′-dicarbaldehyde (**9**) was previously prepared by different routes: (a) Parks, J. E.; Wagner, B. E.; Holm, R. H. *J. Organomet. Chem.* **1973**, *56*, 53−66. (b) Newkome, G. R.; Lee, H.-W. *J. Am. Chem. Soc.* **1983**, *105*, 5956−5957.

(15) Lüning, U.; Müller, M. *Liebigs Ann. Chem.* **1989**, 367−374.

(16) Ortep-3 for Windows: Farrugia, L. J. *J. Appl. Crystallogr.* **1997**, *30*, 565.

(17) Caron, A.; Guilhelm, J.; Riche, C.; Pascard, C.; Alpha, B.; Lehn, J.-M.; Rodriguez-Ubis, J. C. *Helv. Chim. Acta* **1985**, *68*, 1577−1582.

(18) Bkouche-Waksman, I.; Guilhem, J.; Pascard, C.; Alpha, B.; Deschenaux, R.; Lehn, J.-M. *Helv. Chim. Acta* **1991**, *74*, 1163−1170.

(19) Energy levels of the trivalent lanthanoid aquo species: (a) Tb: Carnall, W. T.; Fields, P. R.; Rajnak, K. *J. Chem. Phys.* **1968**, *49*, 4447−4449. (b) Eu: Carnall, W. T.; Fields, P. R.; Rajnak, K. *J. Chem. Phys.* **1968**, *49*, 4450−4455.

(20) Beeby, A.; Clarkson, I. M.; Dickins, R. S.; Faulkner, S.; Parker, D.; Royle, L.; de Sousa, A. S.; Williams, J. A. G.; Woods, M. *J. Chem. Soc., Perkin Trans. 2* **1999**, 493−503.

(21) Deiters, E.; Song, B.; Chauvin, A.-S.; Vandevyver, C. D. B.; Bünzli, J.-C. *New J. Chem.* **2008**, *32*, 1140−1152.

(22) Faulkner, S.; Beeby, A.; Carrie, M.-C.; Dadabhoy, A.; Kenwright, A. M.; Sammes, P. G. *Inorg. Chem. Commun.* **2001**, *4*, 187−190.

(23) Werts, M. H. V.; Jukes, R. T. F.; Verhoeven, J. W. *Phys. Chem. Chem. Phys.* **2002**, *4*, 1542−1548.

(24) Wingx: Farrugia, L. J. *J. Appl. Crystallogr.* **1999**, *32*, 837−848.

(25) SIR92: Altomare, A.; Cascarano, G.; Giacovazzo, C.; Guagliardi, A. *J. Appl. Crystallogr.* **1993**, *26*, 343−350.

(26) Sheldrick, G. M. *SHELX97, Programs for Crystal Structure Analysis*; Institut für Anorganische Chemie der Universität Göttingen: Göttingen, Germany, 1998.